20th International Conference on Structural Mechanics in Reactor Technology (SMiRT 20)
Espoo, Finland, August 9-14, 2009
SMiRT 20-Division V, Paper 1640

On Scale Effects and Mesh Independence in Dynamic Fracture Analysis by Means of the Discrete Element Method

Jorge Daniel Riera[a], Ignacio Iturrioz[b], and Letícia Fleck Fadel Miguel[c]

[a]*Department of Civil Engineering, UFRGS, Porto Alegre, Brazil. jorge.riera@ufrgs.br*
[b]*Department of Mechanical Engineering, UFRGS, Porto Alegre, Brazil. ignacio@mecanica.ufrgs.br*
[c]*Department of Mechanical Engineering, UFRGS, Porto Alegre, Brazil. letffm@ufrgs.br*

Keywords: Fracture, Brittle materials, Size effect, Numerical analysis, Mesh objectivity.

1 ABSTRACT

Numerical predictions of the failure load of large structures, accounting for size effects, require the adoption of appropriate constitutive relations. These relations depend on the size of the elements and on the correlation lengths of the random fields that describe material properties. Previously, the authors proposed expressions for the tensile stress-strain relation of concrete, whose parameters are related to standard properties of the material, such as Young's modulus or its specific Fracture Energy and to size. Simulations conducted for a typical concrete showed that as size increases, the effective stress-strain diagram becomes increasingly linear, with a sudden rupture, while at the same time the CVs of the relevant parameters decrease to negligible values, situation that renders Linear Elastic Fracture Mechanics (LEFM) applicable. However, it was later observed that a hither to unknown problem arises in the analysis of non-homogeneous materials, leading to lack of mesh objectivity: the need to know a priori the degree of fracturing. This should also affect finite element analysis, requiring a careful evaluation of the energy dissipated by fracture or other mechanisms in the course of the loading process. In the paper a tentative criterion is proposed to account for the effect in non-linear dynamic fracture analysis.

2 INTRODUCTION

The authors determined numerically the response of geometrically similar reinforced concrete beams built in four different sizes, tested to rupture by Leonhart and Walter (1961) and later reproduced by Ramallo *et al.* (1995), to quantify size effects in reinforced concrete beams. For such purpose the so-called Discrete Element Method (DEM) was employed, modeling the inhomogeneous character of concrete and steel by assuming that their stiffness and specific fracture energies are random fields in 3D-space. The constitutive criteria, based on Hillerborg's model (1971), presented improvements in the consideration of the spatial correlation of the random fields. The discrete numerical model was also used to reproduce experimental results due to Vliet and Mier (2000) on the influence of sample size on the tensile strength of concrete and the strength of large rock dowels subjected to shear (Miguel *et al.*, 2008). In all cases, in order to represent the stress-strain relation for concrete in tension, a triangular diagram was resorted to, which proved adequate when the size of the elements is sufficiently small and the inhomogeneous properties of the material are properly accounted for. These conditions require large DEM or FEM models, which cannot be usually employed in engineering practice due to cost-effectiveness considerations. In a previous paper Riera and Iturrioz (2007) contend that predictions of the failure load of concrete structures, which account for size effects, can be made using larger elements and therefore reduced computational costs, if the appropriate stress-strain relations are adopted. These relations depend both on the size of the element and on the correlation lengths of the random fields that describe the relevant material properties. The numerical determination of the response of concrete samples ranging in size from 0.20 to 1.60m subjected to uni-axial tension predicted the expected reduction in strength and the increased fragility of the samples as size of the specimens increases, as can be seen in Figure 1. Although comparisons with experimental evidence are quite satisfactory, it was later found that the proposed procedure does not satisfy conditions of mesh objectivity.

In response determinations of structures with initial cracks or high stress gradients, which result in fracture localization, well established procedures lead to results that are mesh independent. However, in

elements subjected to approximately uniform stress fields a hither to unknown problem arises in the analysis of non-homogeneous materials: the need to know *a priori* the degree of fracturing of the element. This should also affect finite element analysis in cases in which there is no clear fracture localization, requiring a careful evaluation of the energy dissipated by fracture or other mechanisms in the course of the loading process. In the paper tentative criteria is proposed to account for the effect in non-linear dynamic fracture analysis of large structural systems.

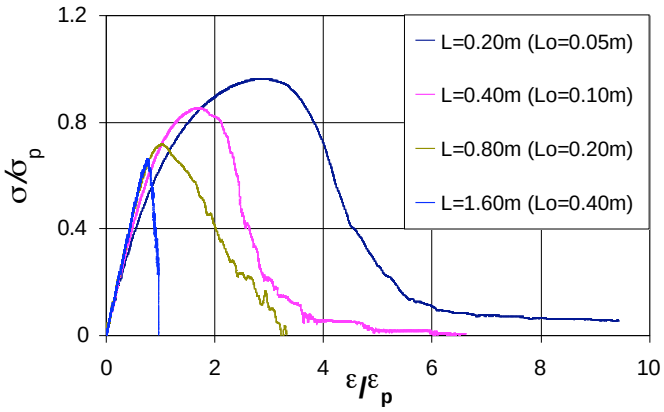

Figure 1: Normalized mean tensile stress *vs.* mean strain in cubic concrete samples [Riera and Iturrioz (2007)].

3 THE DISCRETE ELEMENT METHOD IN FRACTURE PROBLEMS

The Discrete Element Method employed in this paper is based on the representation of a solid by means of an arrangement of elements able to carry only axial loads The equivalence between an orthotropic elastic continuum and the cubic arrangement of uni-axial elements consisting of a cubic cell with eight nodes at its corners plus a central node was shown by Nayfeh and Hefzy (1978). The discrete elements representation of the orthotropic continuum was adopted by the authors to solve structural dynamics problems by means of explicit direct numerical integration of the equations of motion, assuming the mass lumped at the nodes. Each node has three degrees of freedom, corresponding to the nodal displacements in the three orthogonal coordinate directions.

The equivalence between the orthotropic elastic solid with orthotropy axes oriented in the direction parallel to the longitudinal elements of the discrete elements model was extensively verified by Hayashi (1982). The equations that relate the properties of the elements with the elastic constants of an isotropic medium are:

$$\delta = \frac{9\nu}{4-8\nu}\ , \qquad EA_n = EL_0^2\,\frac{(9+8\delta)}{2(9+12\delta)}\ , \qquad EA_d = \frac{2\sqrt{3}}{3}A_n \tag{1}$$

in which E and ν denote Young's modulus and Poisson's ratio, respectively, while A_n and A_d represent the areas of normal and diagonal elements.

The resulting equations of motion may be written in the well-known form:

$$\boldsymbol{M}\ddot{\vec{x}} + \boldsymbol{C}\dot{\vec{x}} + \vec{F}_r(t) - \vec{P}(t) = 0 \tag{2}$$

in which $\vec{x}$ represents the vector of generalized nodal displacements, $\boldsymbol{M}$ the diagonal mass matrix, $\boldsymbol{C}$ the damping matrix, also assumed diagonal, $\vec{F}_r(t)$ the vector of internal forces acting on the nodal masses and $\vec{P}(t)$ the vector of external forces. Obviously, if $\boldsymbol{M}$ and $\boldsymbol{C}$ are diagonal, Equations (2) are not coupled. Then the explicit central finite differences scheme may be used to integrate Equation (2) in the time domain. Since the nodal coordinates are updated at every time step, large displacements can be accounted for in a natural and efficient manner.

In the present paper, the relation between tensile stress and strain in the material was assumed to be triangular. The limit strain ε_r is determined to satisfy the condition that, upon rupture of the element, once the strain reaches the value ε_r, energy U_{elem} is liberated, according to Equation (3):

$$U_{elem} = \frac{A_f G_f}{L_0} \tag{3}$$

in which A_f is the fractured area bar, L_0 is the normal bar length and G_f is the specific fracture energy that characterized the material toughness. Note that the fracture energy, *i.e.*, the energy dissipated by the total rupture of one element, depends on the numerator of Equation (3), which is the product of the fracture area within the element times the specific fracture energy of the material. In previous papers (Rocha, 1989; Riera and Iturrioz, 1998; Miguel *et al.*, 2008), the assumption that A_f equals the area of the basic brick element L_0^2 was implicit. On that basis, the fracture area of the longitudinal bars is given by:

$$A_f = c_a L_0^2 \tag{4}$$

In which the coefficient c_a was computed as 0.1385. For diagonal bars, c_a equals 0.1593. This assumption is valid as long as there is a strong localization effect, leading to a rupture configuration characterized by a single large crack. One such example is fracture of a rock dowel (Miguel *et al.*, 2008), which occurs in most cases as a crack that, starting near the intersection between the dowel wall and the base, propagates through the dowel.

Another important feature of the approach is the assumption that G_f is not constant throughout the structure. In this paper, a Weibull distribution with coefficient of variation of 50% is adopted. It should be underlined again that fracture localization weakens as the non-homogeneous nature of the material becomes more pronounced, *i.e.*, as the coefficients of variation of the fields that describe the material properties increase.

Applications of the DEM in studies involving non-homogeneous materials subjected to fracture, like concrete and rock, may be found in Iturrioz (1995), Riera and Iturrioz (1998), Dalguer *et al.* (2001), Rios (2002) and Miguel *et al.* (2008). Additionally, Dalguer *et al.* (2003), Riera *et al.* (2005), Miguel (2005), Miguel *et al.* (2006) and Miguel and Riera (2007), contributed to demonstrate the reliability of the approach.

4 SIZE EFFECT IN FRACTURE ANALYSIS OF NON-HOMOGENEOUS CUBES

4.1 Uniform Displacement

Initially, concrete cubic samples fixed at the lower face and subjected to tensile stress on the upper face were analyzed up to failure through numerical simulation. The size of the cubes ranges from 0.12m to 0.96m. Cube dimensions and DEM mesh employed in the analysis are indicated in Table 1. The material properties of the concrete are given in Table 2.

Table 1: Basic dimensions of the concrete samples.

Sample size (m)	DEM mesh	L_0 (m)
0.12	6×6×6	0.02
0.24	12×12×12	0.02
0.48	24×24×24	0.02
0.72	36×36×36	0.02
0.96	48×48×48	0.02

Table 2: Concrete properties.

Property	Value
E (Young's modulus)	3.5E10N/m^2
ρ (mass density)	2400kg/m^3
ν (Poisson's ratio)	0.25
E(G_f) (expected value of specific fracture energy)	100N/m
ε_p (critical strain)	6.3E-5
CV(G_f) (coefficient of variation of G_f)	50%

Nodal points on the upper face of the specimens were subjected to a controlled uniform displacement that increases smoothly in time, inducing a nominally uniform tension in the specimen. Six simulations were performed for each size. The resulting stress-strain curves for all simulations of the 0.12m cube are shown in Figure 2. Note that the fracture energy of the material is regarded as a random field with the properties indicated in Table 2 and Weibull (Minimum Type III) probability distribution function, so each simulated test leads to a different stress-strain curve. As expected, the variability of the predicted response decreases when the cube size grows. The mean curve for all simulations is also shown in Figure 2, while the mean curves for all sizes are shown in Figure 3.

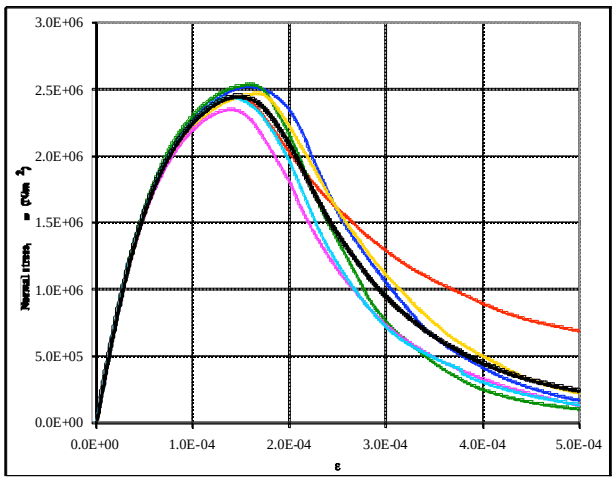

Figure 2: Normal stress on the lower face *vs*. mean strain for the 0.12m cube, for all simulations and resulting mean curve (uniform imposed displacements).

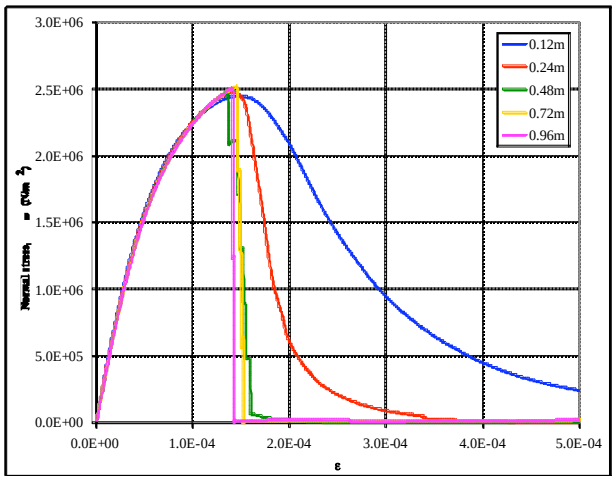

Figure 3: Normal stress on the lower face *vs*. mean strain for the mean curve of all tested sizes (uniform imposed displacements).

A typical crack distribution is shown in Figure 4, corresponding to one simulation for *L=0.72m*. Undamaged, damaged and totally broken elements are represented in cyan, orange and red, respectively. The graphs show both a typical fracture pattern, as well as the damage distribution in the cube. Table 3 presents the average tensile strength and the corresponding strain of the cubes, which are not sensitive to size within the simulation range.

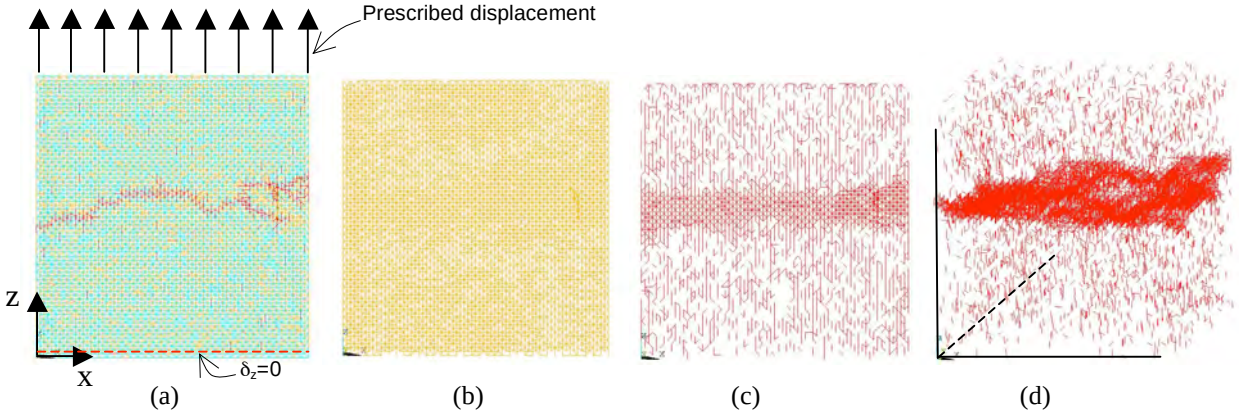

Figure 4: Rupture configuration of L=0.72m simulated sample subjected to uniform prescribed displacements on upper surface: (a) view of rupture configuration, (b) damaged elements, (c) fractured elements, (d) fractured elements in 3D view.

Table 3: Mean peak tensile stress and corresponding strain for uniform imposed displacements**.**

Sample size (m)	Stress σ_r (Mpa)	Strain ε_r
0.12	2.45	1.47E-4
0.24	2.48	1.41E-4
0.48	2.48	1.36E-4
0.72	2.52	1.46E-4
0.96	2.51	1.41E-4

4.2 Triangular Displacement

Next, the concrete simulated samples, fixed at the lower face, were subjected to triangularly distributed displacements with constant strain rate on their upper face and analyzed up to failure through numerical simulation. Again, the size of the cubes ranges from 0.12m to 0.96m and cube dimensions and DEM mesh employed in the analysis are indicated in Table 1. The material properties of the concrete were given in Table 2.

Six simulations were performed for each size, except for the largest sample (0.96m) in which case only two simulations were performed on account of the processing time required (about 30 hours) for each simulation. The resulting stress-strain curves for all simulations of the 0.12m cube are shown in Figure 5, which also presents the mean curve. Direct observation shows that the variability of the predicted response also diminishes when the cube size grows. Figure 6 shows the mean curves for all simulated sample sizes.

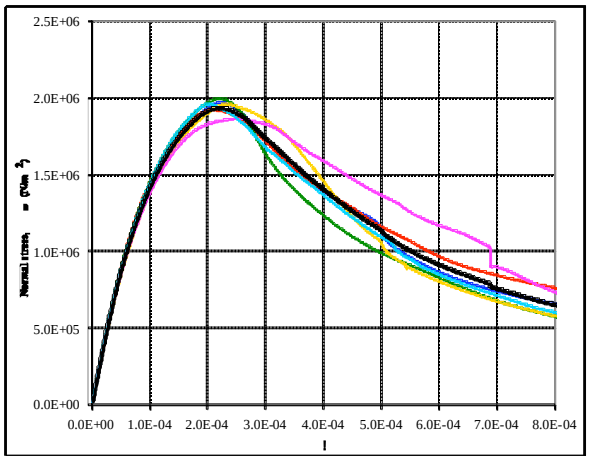

Figure 5: Normal stress on the lower face *vs*. mean strain for the 0.12m cube, for all simulations and resulting mean curve (triangular imposed displacements).

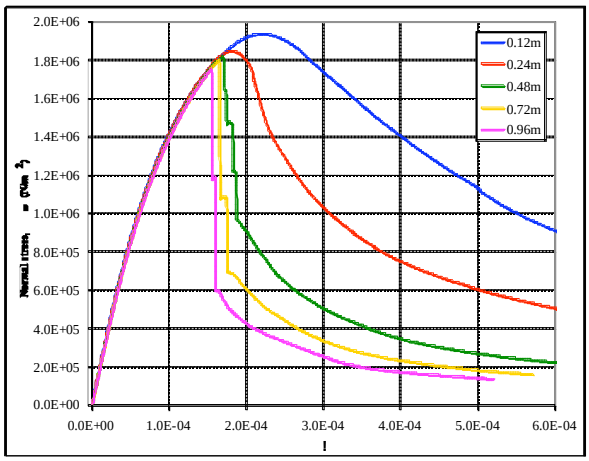

Figure 6: Normal stress on the lower face *vs*. mean strain for the mean curve of all tested sizes (triangular imposed displacements).

Typical crack patterns are shown in Figure 7. Undamaged, damaged and totally broken elements are represented in cyan, orange and red, respectively. The models show both a perceptible size effect as well as typical cracking patterns, *i.e.*, the damage distribution in the cubes. Table 4 presents the average tensile strength and ultimate strain of the cubes, which tend to decrease as the size of the cube increases.

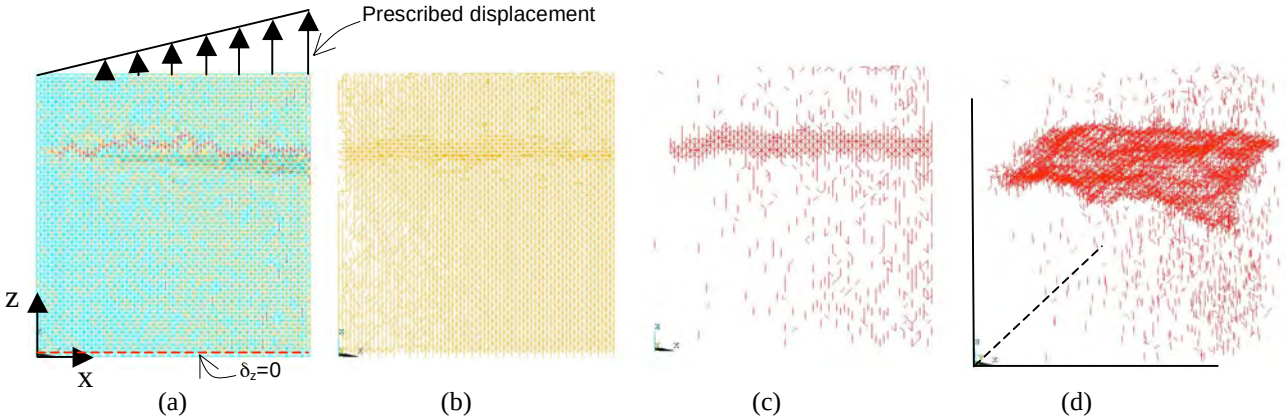

Figure 8: Rupture configuration of L=0.72m simulated sample subjected to triangular prescribed displacements on upper surface: (a) view of rupture configuration, (b) damaged elements, (c) fractured elements, (d) fractured elements in 3D view.

Table 4: Mean peak tensile stress and corresponding strain for triangular imposed displacements.

Sample size (m)	Stress σ_r (Mpa)	Strain ε_r
0.12	1.94	2.20E-4
0.24	1.85	1.80E-4
0.48	1.82	1.69E-4
0.72	1.80	1.64E-4
0.96	1.75	1.55E-4

In Figures 4 and 7 it may be seen that damage localization is more pronounced in presence of a stress gradient (triangular imposed displacements). Both damage, indicated by the orange-tainted regions, as well as crack surfaces are more widely distributed in uniform imposed displacements (Figure 4). Although no experimental results for this size range are known to the authors, the effects unquestionably exist. Therefore, both features of the non-linear problem should be taken into consideration if larger DEM or FEM elements must be resorted to in order to reduce computational costs.

5 SIZE DEPENDENCE OF FRACTURE ENERGY

Table 5 presents data on the variation of the fracture energy needed to split the specimen in two parts as its size increases. The first column presents the theoretical minimum energy E_{min} , while the second column shows the energy determined by simulation for a nominal uniform stress (or strain) distribution. It was also observed that for triangular applied displacements, the fracture energy approaches the theoretical minimum, indicating a strong localization effect.

Table 5: Fracture energy needed to split the specimen in two parts in a nominally uniform strain field.

Size (m)	E_{min} (Nm)	E_{num} (Nm)	E_{num}/E_{min}
0.12	1.44	1.69	1.17
0.24	5.76	6.85	1.19
0.48	23.04	27.72	1.20
0.72	51.84	76.38	1.47
0.96	92.16	167.0	1.81

The results in Table 5 imply that if larger DEM elements are employed in fracture studies, in addition to the stress-strain diagram associated to the element size, the correct c_a coefficient must be used, which is obtained by multiplying the value 0.1385 [see eq.(4)], calculated on the assumption of a single crack across the element by the coefficient in the last column of Table 5. This correction would allow considering the occurrence of additional damage, beyond the failure surface, as shown by Figure 4. Carpinteri and Chaia (2002) consider this effect by introducing the notion of fractal dimension, linked to fractured area as defined in this study, when the fractal dimension is higher than 2 (d=2.3).

6 CONCLUSIONS

It was confirmed in this examination of the tensile fracture behavior of concrete cubes that predictions of fracture of non-homogeneous materials using DEM models are feasible and yield results that are consistent with the experimental evidence so far available. The use of large elements, in which extensive cracking within the elements of the model may be expected, requires the consideration of the increase with size of the fractured area, in addition to the effective stress-strain curve for the element. This is a basic requirement in order to achieve mesh objectivity. Note that the degree of damage localization must be known *a priori*, which is a still unresolved difficulty of the nonlinear fracture analysis of nonhomogeneous large structures. In addition, the influence of internal damping (not due to fracture, which is accounted for) in the numerical dynamic response analysis must also be verified and constitutes a line of ongoing research at PPGEC/PROMEC, UFRGS.

Acknowledgements. *The authors acknowledge the support of CNPq and CAPES (Brazil).*

REFERENCES

Carpinteri, L., and Chiaia, B., Embrittlement and decrease of apparent strength of large-sized concrete structures. *Sadhana*, Vol. 27, Part 4, August 2002, 425-448, India.

Dalguer, L. A., Irikura, K., Riera, J. D., and H. C. Chiu, The importance of the dynamic source effects on strong ground motion during the 1999 Chi-Chi, Taiwan, earthquake: Brief interpretation of the damage distribution on buildings. *Bull. Seismol. Soc. Am*., 91, 1112-1127, 2001.

Dalguer, L. A., Irikura, K., and Riera, J. D., Simulation of tensile crack generation by three-dimensional dynamic shear rupture propagation during an earthquake. *J. Geophys. Res.*, 108(B3), 2144, 2003.

Hayashi, Y., Sobre uma representação discreta de meios contínuos em dinâmica não-linear. *M. S. thesis*, CPGEC, Universidade Federal do Rio Grande do Sul, Porto Alegre, Brazil, 1982.

Hillerborg, A., A model for fracture analysis, Cod. LUTVDG/TVBM 300-51-8, 1971.

Iturrioz, I., Aplicação do método dos elementos discretos ao estudo de estruturas laminares de concreto armado. *Ph.D. thesis*, CPGEC, Universidade Federal do Rio Grande do Sul, Porto Alegre, Brazil, 1995.

Leonhart, F. and Walker, R., The Stuttgart shear tests, Translation No. 11, C&CA, London. *Beton und Stahlbetonbau*, Vol. 65, no. 12, 1961, Vol. 57, No. 2, 3, 7 & 8, 1961.

Miguel, L. F. F., Critério constitutivo para o deslizamento com atrito ao longo da falha sísmica. *Ph.D. thesis*, 229 pp., PPGEC, Escola de Engenharia, Universidade Federal do Rio Grande do Sul, Porto Alegre, Brazil, 2005.

Miguel, L. F. F., Riera, J. D., and Dalguer, L. A., Macro constitutive law for rupture dynamics derived from micro constitutive law measured in laboratory. *Geophys. Res. Lett*., 33, L03302, 2006, doi:10.1029/2005GL024912.

Miguel, L. F. F., and Riera, J. D., A constitutive criterion for the fault: modified velocity-weakening law. *Bull. Seismol. Soc. Am.*, 97(3), 915-925, 2007, doi:10.1785/0120060107.

Miguel, L. F. F., Riera, J. D., and Iturrioz, I., Influence of size on the constitutive equations of concrete or rock dowels. *International Journal for Numerical and Analytical Methods in Geomechanics*, Vol. 32, No. 15, pp. 1857-188, 2008. DOI: 10.1002/nag.699.

Nayfeh, A. H., and Hefzy, M. S., Continuum modeling of three-dimensional truss-like space structures. *AIAA Journal*, 16(8), 779-787, 1978.

Ramallo, J. C., Kotsovos, M. D., and Danesi, R. D. Unintended out-of-plane actions in size effects tests of structural concrete, *Transactions, 13th Int. Conf. on Structural Mech. in Reactor Tech*. (SMiRT 13), Vol. 3, 351-357, 1995.

Riera, J. D., and Iturrioz, I., Discrete elements model for evaluating impact and impulsive response of reinforced concrete plates and shells subjected to impulsive loading. *Nuclear Engineering and Design*, 179, 135-144, 1998.

Riera, J. D., and Iturrioz, I., Size effects in the analysis of concrete or rock structures. Paper presented at SMiRT 19: *International Conference on Structural Mechanics in Reactor Technology*, 2007.

Riera, J. D., Miguel, L. F. F., and Dalguer, L. A., On the constitutive criteria for the fault: Influence of size and tensile cracks generation during rupture. Paper presented at SMiRT 18: *International Conference on Structural Mechanics in Reactor Technology*, Beijing, China, 2005.

Rios, R. D., Aplicações do método dos elementos discretos em estruturas de concreto. *Ph.D. thesis*, PPGEC, Universidade Federal do Rio Grande do Sul, Porto Alegre, Brazil, 2002.

Rocha, M. M., Ruptura e efeitos de escala em materiais não-homogeneos. *M. S. thesis*, CPGEC, Universidade Federal do Rio Grande do Sul, Porto Alegre, Brazil, 1989.

Van Vliet, M. R. A, Van Mier, J. G. M, Size effects of concrete and sandstone, *HERON*, Vol 45, No.2, 91-108, 2000.